Polarization entanglement with graded-index lenses

Giuseppe Vallone,[1,2,a),b)] Gaia Donati,[2,b)] Francesco De Martini,[2,3,b)] and Paolo Mataloni[2,4,b)]
[1]*Museo Storico della Fisica e Centro Studi e Ricerche "Enrico Fermi," Via Panisperna 89/A, Compendio del Viminale, Roma 00184, Italy*
[2]*Dipartimento di Fisica, Sapienza Università di Roma, Roma 00185, Italy*
[3]*Accademia Nazionale dei Lincei, via della Lungara 10, Roma 00165, Italy*
[4]*Istituto Nazionale di Ottica Applicata (INOA-CNR), L.go E. Fermi 6, 50125 Florence, Italy*

(Received 29 July 2009; accepted 8 October 2009; published online 6 November 2009)

By using an optical device based on the integration of a graded-index (GRIN) rod lens and a single-mode optical fiber we efficiently collected photon pairs generated by spontaneous parametric down-conversion. We show that this system preserves the polarization entanglement of the two-photon states. Hence this device, characterized by a remarkable easiness of alignment and allowing for high coupling efficiency of single-mode radiation, can be used with photons entangled in various degrees of freedom, such as polarization and spatial momentum and to interconnect different sides of complex optical circuits. © *2009 American Institute of Physics*.
[doi:10.1063/1.3257376]

Photon entanglement is a key resource for modern quantum information (QI) applications such as quantum computation[1,2] and communication protocols.[3,4] Spontaneous parametric down-conversion (SPDC) is up to now the most established technique to generate photon entanglement by using polarization and other degrees of freedom (DOFs) of the photons.[5–13] The realization of four[14] and six-photon[15] entangled states together with the introduction of hyperentangled states,[16–18] based on the entanglement of two photons in many DOFs (such as polarization and longitudinal momentum), open important perspectives in the implementation of QI tasks with multiqubit photon states.

In a recent letter,[9] we have demonstrated the entanglement of two photons in many optical modes by collecting the degenerate conical SPDC radiation (with horizontal polarization) of a type I phase-matched crystal. Multipath entanglement was realized by a set of graded-index (GRIN) lenses, carefully aligned in the annular section of the SPDC cone and efficiently connected to a bundle of single-mode optical fibers. This experiment proved the feasibility of using GRIN lenses with longitudinal momentum entanglement and thus suggests to test the entanglement in other DOFs, such as polarization. In particular, the absence of any birefringence effect, introducing a polarization decoherence due to temporal and/or spatial walk-off in the GRIN lenses, should be verified.

In this letter, we investigate the polarization performances of the integrated device composed of a GRIN rod lens and a single-mode optical fiber. We focus on the preservation of polarization entanglement. This result, together with the high collection efficiency, the easiness of alignment, and the low translational sensitivity, makes this optical integrated system a powerful tool for advanced QI tasks.

The basic elements of the optical device we are going to consider are a single-mode fiber (SMF; Thorlabs,[19] mod. P1–630A-FC-2) and a "quarter-pitch" GRIN rod lens (GL; Grintech,[20] mod. GT-LFRL-200–025–50-NC(728), length =5.0 mm, diameter=2.0 mm, numerical aperture=0.5, anti-reflection (AR)-coated on the input face). We recall that the term "quarter-pitch" refers to the GRIN lens length, chosen in such a way that an input plane wave is focused on the output face of the GRIN lens.

The GL is glued to one end of the fiber to give the definitive integrated optical system, from here on labeled as GL-SMF. The coupling efficiency of a GL-SMF system is essentially determined during the fixing procedure of the two components. The latter was performed by using a continuous wave (cw), horizontally polarized Ti:Sapphire laser beam ($\lambda_{Ti:Sa}$=728 nm), which simulates the input radiation collected by the two GL-SMF systems included in the experimental setup. A positive lens (focal length 500 mm) was

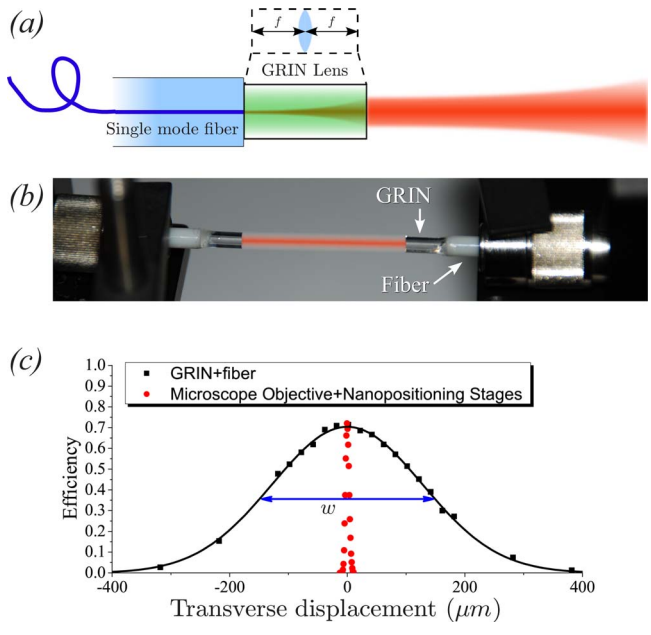

FIG. 1. (Color online) (a) Sketch of the GL-SMF system lying within the confocal parameter of the input mode. (b) Picture of two GL-SMF systems put face to face. Each GRIN lens is glued to the input face of the corresponding single-mode optical fiber. (c) Comparison between the collection efficiency of a GL-SMF (black curve) and a 40× objective as a function of transverse displacement. $w=(301\pm4)\mu m$ is the full width at half maximum of the Gaussian fitting curve.

a)Electronic mail: giuseppe.vallone@uniroma1.it.
b)URL: http://quantumoptics.phys.uniroma1.it/

 © 2009 American Institute of Physics

Author complimentary copy. Redistribution subject to AIP license or copyright, see http://apl.aip.org/apl/copyright.jsp

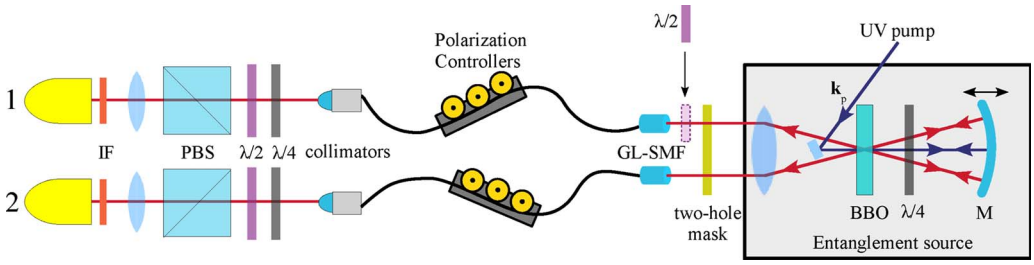

FIG. 2. (Color online) Experimental setup used for polarization Bell-state measurements. The basic elements of the entanglement source are described in Ref. 21.

inserted in the Ti:Sa beam path to model the beam shape and let the beam waist coincide with the location of the GL. This choice approximately sets the optimal coupling conditions for the radiation entering the GL-SMF system. As shown in Fig. 1(a), the considered GRIN lens is equivalent to a lens with focal length $f \simeq 2$ mm (here $f=\frac{1}{n_0 g}$, where n_0 is the maximum value of the index of refraction within the GRIN lens and $g=0.312$ mm^{-1} is its gradient constant[20]) and two free space propagations of length f. Hence it is possible to describe the coupled beam in terms of its beam waist $W_0' \simeq \frac{\lambda}{\pi W_0} f \simeq 185$ μm and the corresponding confocal parameter $z_0'=\frac{\pi W_0'^2}{\lambda} \simeq 150$ mm. These values can be calculated from the core diameter of the fiber ($2W_0 \simeq 5$ μm, see[19]).

First, we aligned the input face of the GL orthogonal to the laser beam with its AR-coated side turned to the input radiation in order to avoid reflections. We then brought the SMF closer to the GL and optimized the coupling into the fiber. By knowing the input power, it was possible to obtain the optimal coupling conditions by monitoring the collection efficiency of each GL-SMF system (calculated as P_{out}/P_{in}) and improve it by submicrometric displacements and careful tilting of the fiber. Once the GL and the SMF were sufficiently close to each other, we proceeded to glue the two components. A coupling efficiency of almost 70% and a Gaussian shape translational efficiency with full width at half maximum equal to $w=(301 \pm 4)$ μm were measured for the two integrated systems built by this procedure.

Successively, the two equal GL-SFM systems were used to collect polarization-entangled photon pairs generated by a SPDC source. The source, shown in Fig. 2, and described in another letter,[21] generates the polarization-entangled state

$$|\Phi^\theta\rangle = \frac{1}{\sqrt{2}}(|H\rangle_1|H\rangle_2 + e^{i\theta}|V\rangle_1|V\rangle_2), \quad (1)$$

over two modes selected from the degenerate emission cone of a type I β-barium-borate crystal. The selected SPDC radiation was then collected by the two GL-SMF systems. For each SMF, a manual polarization controller (PC) allowed to invert the unitary transformation introduced by the fiber. Finally, two standard polarization-analyzer settings constituted by a $\lambda/4$ wave-plate, a $\lambda/2$ wave-plate, and a polarizing beam splitter allowed the characterization of the output radiation focused on two single-photon detectors (Perkin-Elmer, mod. SPCM-AQR14), labeled as 1 and 2 in Fig. 2. Two interference filters (IF; bandwidth $\Delta\lambda$) placed in front of the detectors determine the coherence time of the emitted photons; in the present experiment we considered two different values of the bandwidth, namely $\Delta\lambda=6$ nm and $\Delta\lambda=70$ nm. With the former (latter) choice we obtained nearly 180 coinc/s (1000 coinc/s) within a coincidence window of 3 ns. This determines a coincidences/singles ratio of almost 8%.

By varying the position of the spherical mirror M (shown in Fig. 2), we were able to change the relative phase θ in the generated state $|\Phi^\theta\rangle$. We measured the photon coincidence rate as a function of the mirror position with the polarization analyzers set to diagonal polarizations, i.e., we detected both photons with polarization $\frac{1}{\sqrt{2}}(|H\rangle+|V\rangle)$. The experimental results are shown in Fig. 3 for the two bandwidth values $\Delta\lambda$ of the IFs. In our experimental conditions, the $\Delta\lambda=70$ nm IFs were used to filter out stray-light radiation. In this case, the actual bandwidth of the detected photons is narrower than 70 nm because of the two following effects: the spatial mode selection operated by the SMFs and the presence of position-frequency correlations characteristic of the SPDC radiation.

The variation of the number of coincidences N_C with the phase θ is precisely the one expected for entangled states such as $|\Phi^\theta\rangle$, $N_C(|\Phi^\theta\rangle) \propto 1+\cos\theta$. The coincidence fringe visibility reaches the value $V=0.9785 \pm 0.0001$ for $\Delta\lambda=6$ nm, while $V=0.9094 \pm 0.0001$ for $\Delta\lambda=70$ nm. The maxima and minima of these interference patterns single out the longitudinal positions of the mirror M corresponding to the Bell states $|\Phi^+\rangle=\frac{1}{\sqrt{2}}(|H\rangle_1|H\rangle_2+|V\rangle_1|V\rangle_2)$ and $|\Phi^-\rangle=\frac{1}{\sqrt{2}}(|H\rangle_1|H\rangle_2-|V\rangle_1|V\rangle_2)$, respectively. The slight difference between the two fringe pattern periods in Fig. 3 is mainly due to the different bandwidth values.

The tomographic reconstruction of the coupled radiation represents the primary instrument to evaluate the polarization performances of the GL-SMF setup. Besides the two Bell states cited above, which are derived from the original generated entangled state $|\Phi^\theta\rangle$ by appropriately setting the mirror M position, we can obtain $|\Psi^\pm\rangle=\frac{1}{\sqrt{2}}(|H\rangle_1|V\rangle_2 \pm |V\rangle_1|H\rangle_2)$ thanks to an additional $\lambda/2$ wave-plate placed in front of one of the integrated GL-SMF systems. Figure 4 shows the results of the four tomographic characterizations, with the ele-

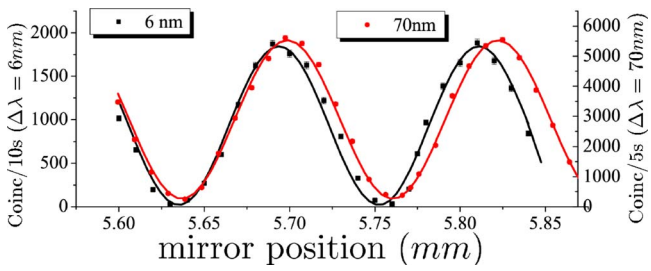

FIG. 3. (Color online) Coincidence rate measured as a function of the mirror M position for $\Delta\lambda=6$ nm (black curve) and $\Delta\lambda=70$ nm (red curve).

Author complimentary copy. Redistribution subject to AIP license or copyright, see http://apl.aip.org/apl/copyright.jsp

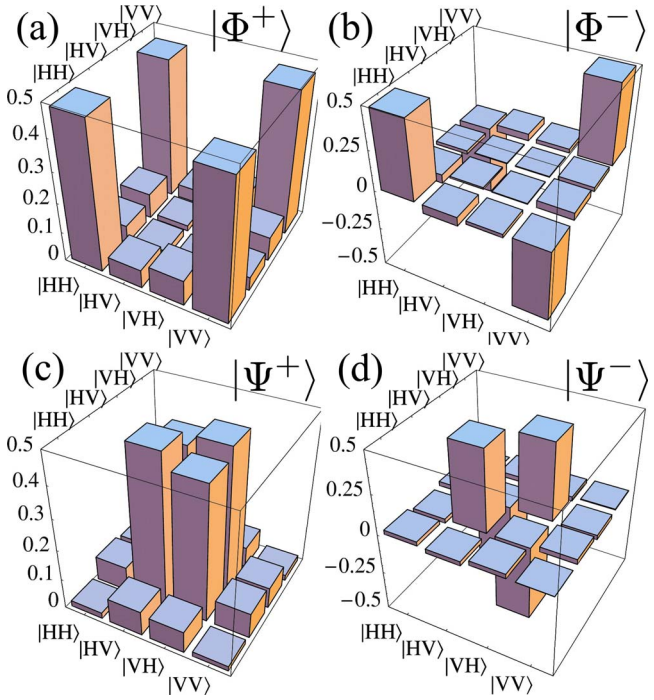

FIG. 4. (Color online) Tomographic reconstruction of the four polarization-entangled generated states (real parts). A maximum likelihood technique was used to obtain physical density matrices. The imaginary components are negligible. The corresponding theoretical Bell states are: (a) $|\Phi^+\rangle$, (b) $|\Phi^-\rangle$, (c) $|\Psi^+\rangle$, and (d) $|\Psi^-\rangle$.

ments of the density matrices written in the polarization basis $\{|HH\rangle, |HV\rangle, |VH\rangle, |VV\rangle\}$.

For every generated state, we note the presence of the characteristic diagonal terms and the strong coherences (with negative signs when looking to the singlet state $|\Psi^-\rangle$ and to $|\Phi^-\rangle$) existing between them. The fidelities of the experimental states are: $F_{|\Phi^+\rangle}=0.938\pm0.019$, $F_{|\Phi^-\rangle}=0.949\pm0.020$, $F_{|\Psi^+\rangle}=0.923\pm0.014$, and $F_{|\Psi^-\rangle}=0.965\pm0.029$, all of which show a strong closeness to the theoretical Bell states (encoded in polarization). A more quantitative parameter associated to the generated polarization-entangled states is given by the tangle τ: $\tau_{|\Phi^+\rangle}=0.873$, $\tau_{|\Phi^-\rangle}=0.940$, $\tau_{|\Psi^+\rangle}=0.846$, and $\tau_{|\Psi^-\rangle}=0.911$. These values are the evidence of a high degree of entanglement generation.

We presented a device built as an integrated system of a GRIN lens glued to a single-mode optical fiber. In the present letter we have shown that this system preserves polarization entanglement of SPDC radiation, despite possible anisotropies between the radial and tangential components of the mode.[22] Since this very device gave successful results when used with longitudinal momentum entanglement,[9] it can be adopted for a series of QI applications where different types of entanglement are involved. Particularly, it could be a useful instrument to connect different sides of complex optical circuits.

When thinking of future applications involving optical microchips, it is worth investigating the possible solutions to link distinct elements in order to perform more complex operations.[23–25] For this purpose we studied the coupling efficiency of the sequence of two GL-SMF systems separated by a variable path in free space and set out as pictured in Fig. 1(b). For a free space separation changing from 1 to 40 mm we measured a coupling efficiency of almost 90%.

This work was supported by Finanziamento Ateneo 2008 (prot. C26A08RMYF) of Sapienza Università di Roma. Thanks to L. Businaro and R. Ursin for useful discussions and to M. Figliuzzi and A. Rossi for their support in the preparation of the experiment.

[1] E. Knill, R. Laflamme, and G. J. Milburn, Nature (London) **409**, 46 (2001).
[2] R. Raussendorf and H. J. Briegel, Phys. Rev. Lett. **86**, 5188 (2001).
[3] C. H. Bennett and G. Brassard, *Proceedings of the IEEE International Conference on Computers, Systems and Signal Processing*, Bangalore, India (IEEE, New York, 1984), p. 175.
[4] A. K. Ekert, Phys. Rev. Lett. **67**, 661 (1991).
[5] P. G. Kwiat, K. Mattle, H. Weinfurter, A. Zeilinger, A. V. Sergienko, and Y. Shih, Phys. Rev. Lett. **75**, 4337 (1995).
[6] P. G. Kwiat, E. Waks, A. G. White, I. Appelbaum, and P. H. Eberhard, Phys. Rev. A **60**, R773 (1999).
[7] J. G. Rarity and P. R. Tapster, Phys. Rev. Lett. **64**, 2495 (1990).
[8] A. Mair, A. Vaziri, G. Weihs, and A. Zeilinger, Nature (London) **412**, 313 (2001).
[9] A. Rossi, G. Vallone, A. Chiuri, F. De Martini, and P. Mataloni, Phys. Rev. Lett. **102**, 153902 (2009).
[10] J. T. Barreiro, N. K. Langford, N. A. Peters, and P. G. Kwiat, Phys. Rev. Lett. **95**, 260501 (2005).
[11] E. Nagali, F. Sciarrino, F. De Martini, L. Marrucci, B. Piccirillo, E. Karimi, and E. Santamato, Phys. Rev. Lett. **103**, 013601 (2009).
[12] J. D. Franson, Phys. Rev. Lett. **62**, 2205 (1989).
[13] J. Brendel, N. Gisin, W. Tittel, and H. Zbinden, Phys. Rev. Lett. **82**, 2594 (1999).
[14] P. Walther, J.-W. Pan, M. Aspelmeyer, R. Ursin, S. Gasparoni, and A. Zeilinger, Nature (London) **429**, 158 (2004).
[15] C.-Y. Lu, X.-Q. Zhou, O. Gühne, W.-B. Gao, J. Zhang, Z.-S. Yuan, A. Goebel, T. Yang, and J.-W. Pan, Nat. Phys. **3**, 91 (2007).
[16] P. G. Kwiat, J. Mod. Opt. **44**, 2173 (1997).
[17] M. Barbieri, C. Cinelli, P. Mataloni, and F. De Martini, Phys. Rev. A **72**, 052110 (2005).
[18] G. Vallone, E. Pomarico, P. Mataloni, F. De Martini, and V. Berardi, Phys. Rev. Lett. **98**, 180502 (2007).
[19] Technical data of the optical fibers used in the experiment are available at the THORLABS website, http://www.thorlabs.com.
[20] Technical data of the graded index lenses used in the experiment are available at the GRINTECH website, http://www.grintech.de.
[21] C. Cinelli, G. Di Nepi, F. De Martini, M. Barbieri, and P. Mataloni, Phys. Rev. A **70**, 022321 (2004).
[22] D. Tentori and J. Camacho, Appl. Opt. **42**, 4452 (2003).
[23] A. Politi, M. J. Cryan, J. G. Rarity, S. Yu, and J. L. O'Brien, Science **320**, 646 (2008).
[24] G. D. Marshall, A. Politi, J. C. F. Matthews, P. Dekker, M. Ams, M. J. Withford, and J. L. O'Brien, Opt. Express **17**, 12546 (2009).
[25] B. J. Smith, D. Kundys, N. Thomas-Peter, P. G. R. Smith, and I. A. Walmsley, arXiv:0905.2933v2, (unpublished).

Author complimentary copy. Redistribution subject to AIP license or copyright, see http://apl.aip.org/apl/copyright.jsp